The University of Manitoba

A PROTON MAGNETIC RESONANCE STUDY OF THE HINDERED ROTATION IN α,α,2,4,6-PENTACHLOROTOLUENE

by

Bryan John Fuhr

A Thesis

Submitted to

the Faculty of Graduate Studies and Research

University of Manitoba

in Partial Fulfillment

of the Requirements for the Degree

MASTER OF SCIENCE

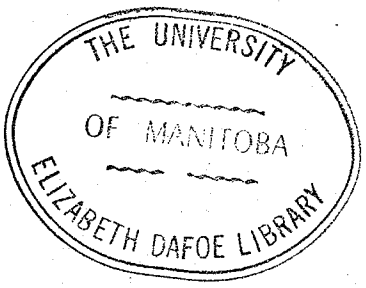

Winnipeg, Manitoba

July, 1969

TO MY PARENTS

ACKNOWLEDGEMENTS

I would like to thank Dr. T. Schaefer for his assistance and many helpful discussions during the past year.

I am also grateful to Dr. Chris Macdonald who helped to prepare the compound studied in the present work, and to Bruce Goodwin who carried out all the computer work involved in this project.

Thanks are also due to Dr. H.M. Hutton and to my colleague Rod Wasylishen for many helpful discussions.

Finally, I am indebted to the National Research Council of Canada for financial support.

ABSTRACT

A proton magnetic resonance study was carried out on the hindered rotation of the dichloromethyl group in α,α,2,4,6-pentachlorotoluene. Two solvents, toluene-d_8 and methylcyclohexane, were used. Rate constants were determined by fitting experimental spectra, obtained over a temperature range of -20° to 70°C, to computer-calculated spectra using linewidth measurements. An effective transverse relaxation time was estimated from the linewidth of a related compound present as an impurity and the variation in relative shift with temperature in the toluene-d_8 solution was accounted for by an extrapolation from lower temperatures.

The activation parameters for the process were calculated from Arrhenius-type plots and from absolute reaction rate theory. Values for the enthalpy of activation were 14.6 ± 1.3 and 13.7 ± 2.2 kcal/mole for the toluene-d_8 and methylcyclohexane solutions respectively. The corresponding values for the free energy of activation were 14.9 ± 0.1 at 30.3°C and 15.0 ± 0.2 kcal/mole at 30.7°C. Both statistical and systematic error limits were estimated (the larger systematic ones are quoted above). The mechanism for the rate process was discussed in the light of the experimental evidence and an attempt was also made to account for the magnitudes of the activation parameters.

TABLE OF CONTENTS

LIST OF TABLES

LIST OF FIGURES

CHAPTER I

Introduction

Nuclear magnetic resonance (NMR) is a useful tool for the study of such rate processes as proton exchange, conformational equilibria and hindered internal rotation. If the rate constants for these processes are comparable in magnitude to the total spread of the NMR spectra (10^{-1} to 10^{5} sec^{-1}) profound changes in the shape of the signals may result from changes in the rate. This line-shape change is the criterion for the study of rate processes. There are several good reviews which cover most aspects of this field in some detail (1-4).

Take as an example the case of two uncoupled nuclei in different environments. Assume that because of some rate process the nuclei are exchanging sites. If the rate of exchange is very slow (the lifetime, τ, of a nucleus at a particular site is long), each nucleus will precess at its own particular Larmor frequency and so two sharp resonance signals separated by a characteristic chemical shift difference, $\delta\nu_{AB}$, will be observed. As the lifetime becomes shorter the resonance peaks will broaden as a consequence of the uncertainty principle. The broadening limit is reached when the lifetime is comparable to the chemical shift difference between the two sites, at which point the two peaks coalesce. A further increase in the exchange rate is indicated by a progressive narrowing of the single peak. Each nucleus no longer has time to change phase at random between successive exchanges and thus only an average magnetic field acts on each nucleus. The limit of this line narrowing is determined by the magnetic field homogeneity of the spectrometer.

A great many rate studies have been carried out using NMR. Unfortunately the quantitative results which were obtained in the past were not very reliable even though many workers claimed optimistic error limits. The numerous conflicting results obtained for cyclohexane ring inversion and the hindered internal rotation in amides (4) confirm the preceding statement. Two main origins of the difficulties in obtaining reliable quantitative results are:

1. Dynamic parameters are very susceptible to spurious effects such as field inhomogeneities or saturation.
2. The theoretical treatment of the experimental data has in many cases been inadequate, mainly because approximate formulae were applied instead of the more complicated complete line-shape theory.

In the subsequent discussion the main points of relaxation and the Bloch equations will be briefly reviewed since they form the basis for the early, classical line-shape theories. The quantum mechanical approach based on density matrices will then be discussed somewhat more fully. The methods for extracting activation parameters from the data will be mentioned and finally the various sources of error involved in the procedure will be reviewed.

CHAPTER II

Theoretical Discussion

A. Relaxation and the Bloch Equations

Consider a nucleus of spin $\underline{I}$ and magnetic moment $\underline{\mu} = \gamma\underline{I}$, where γ is the magnetogyric ratio, subjected to a steady magnetic field $\underline{H}_o$ in the Z-direction. Classically $\underline{\mu}$ precesses about $\underline{H}_o$ with angular frequency $\underline{\omega}_o = \gamma\underline{H}_o$, where the vector $\underline{\omega}_o$ is in the negative Z-direction (assuming $\gamma > 0$). This angular frequency is called the Larmor frequency. For an assembly of nuclei the individual moments add to give a total magnetization $\underline{M}$, but since their phases are randomly oriented, only the Z-component, which is denoted by M_0, will be non-zero.

Now if a radiofrequency field $\underline{H}_1$, rotating in the x-y plane at angular frequency $\underline{\omega}$ in the same direction as $\underline{\omega}_o$, is applied, the individual moments will precess in phase and the x and y-components of $\underline{M}$ will no longer be zero. This perturbation also causes (for spin 1/2 nuclei) the individual z-components of the moments to invert thus tending to equalize the population difference of the two energy levels.

The classical expression:

$$\frac{d\underline{M}}{dt} = \gamma(\underline{M} \times \underline{H}) \qquad \ldots \qquad \ldots \qquad (2\text{-}1)$$

describes the effect of the total field on the magnetization vectors. The component equations of (2-1) referred to a reference frame rotating at angular frequency ω about the z-axis can be shown to be (5)

$$\frac{du}{dt} = (\omega - \omega_o)\, v$$

$$\frac{dv}{dt} = -(\omega_o - \omega)\, u + \gamma H_1 M_z \qquad \ldots \qquad \ldots \qquad (2\text{-}2)$$

$$\frac{dM_z}{dt} = -\gamma H_1 v$$

where u and v are the x and y-components of $\underline{M}$ in the rotating reference frame.

The total magnetization is further influenced by two relaxation processes. The first of these, spin-lattice or longitudinal relaxation, causes M_z to decay to its equilibrium value M_o with a characteristic time T_1. The second process, spin-spin or transverse relaxation, causes u and v to decay to zero; that is, it tends to make the individual moments lose their phase coherence in a characteristic time T_2. More complete discussions of the mechanism for relaxation may be found in various sources (3,6,7).

Equations (2-2) are modified by relaxation terms to yield

$$\frac{du}{dt} = (\omega_o-\omega)v - \frac{u}{T_2}$$

$$\frac{dv}{dt} = -(\omega_o-\omega)u + \gamma H_1 M_z - \frac{v}{T_2} \qquad \ldots \qquad (2\text{-}3)$$

$$\frac{dM_z}{dt} = -\gamma H_1 v - \frac{(M_z-M_o)}{T_1}$$

The above equations are known as the Bloch equations (8) and a fairly detailed derivation of them together with their steady-state solutions may be found in reference (5).

NMR spectrometers are built in such a way as to detect changes in the x-y magnetization which may be written in complex form as

$$G = u + iv \qquad \ldots \qquad (2\text{-}4)$$

The in-phase component, u, corresponds to the dispersion mode and the out-of-phase component, v, corresponds to the absorption mode. It can be shown classically (3) that the power absorbed

(assuming no saturation) is

$$W = \frac{\omega\gamma H_1^2 M_o T_2}{1 + T_2^2 (\omega_o - \omega)^2} \qquad (2\text{-}5)$$

This expression resembles the familiar Lorentz line-shape equation (5). From equation (2-5) is easily derived the formula for the linewidth at half-height of a resonance peak. It is

$$\Delta\omega_{\frac{1}{2}} = \frac{2}{T_2} \quad \text{(in radians/sec)}$$

$$\Delta\nu_{\frac{1}{2}} = \frac{1}{\pi T_2} \quad (\text{in } H_z) \quad ,,, \qquad (2\text{-}6)$$

where $\Delta\nu_{\frac{1}{2}}$ is the linewidth at half-height (in H_z).

B. Rate Processes

1. Early Line-Shape Theories

All the early classical line-shape theories were based on the Bloch equations. The first treatment of the two-site exchange problem was undertaken by Gutowsky, McCall and Slichter (9) and was later elaborated on by Gutowsky and Saika (10) and Gutowsky and Holm (11). The last paper contains the most widely used equations and approximations, but the general theory used is usually referred to as the GMS theory. Essentially in all treatments the Bloch equations were modified to take into account the exchange effects and were then solved directly.

A simpler treatment was worked out by McConnell (12) who generalized the Bloch equations directly to include exchange effects. In this way the previous, involved derivations were reduced to simple algebraic operations, and furthermore the treatment of saturation effects could be incorporated.

Generally the complete line-shape expressions derived from the GMS theory are not used directly, since various approximate formulae have been deduced from them in order to calculate rate constants. These approximations include the following:

1. Change in peak separation in the slow exchange region below coalescence (11).
2. Measurement of the intensity ratio between the two maxima and central minimum of the spectrum below coalescence (13).

3. Measurement of line broadening in the slow exchange region (14,15).
4. Measurement of line narrowing in the fast exchange region (16).
5. Determination of the coalescence temperature from which the rate constant may be deduced (4).

These methods have been widely used in the past, but in many cases they have been employed in situations where the theory does not apply. One such example is the use of the GMS theory in cases where there is strong coupling between the two exchanging protons. In cases where there is only weak coupling, good fits have been obtained (17), but as a rule the generation of the complete line-shape using the quantum mechanical approach is much the superior method. It can easily include AB systems with strong coupling as well as more complicated spin systems.

2. Quantum mechanical Line-shape Theory.

This theory which was first given by Kaplan (18) and extended by Alexander (19) and Whitesides (20) is based on the density matrix formalism (21-23). Several other slightly different approaches have been taken since then (4,24,25). It is not the purpose here to derive the basic theory or apply it in detail to a particular case, since most of this work has been done in the above references. Furthermore the theory and computer program which was used for calculating the rate constants in the present ABX case, have been derived (26) using Whitesides' approach. A very brief outline of this basic approach as it applies to a simple exchanging AB system will now be given.

A list of the important equations from density matrix theory used in the following outline may be found in appendix I.

First of all, the spin product functions used as the basis set for the AB case are

$$\phi_1 = \alpha\alpha$$
$$\phi_2 = \alpha\beta \qquad \ldots. \qquad (2\text{-}7)$$
$$\phi_3 = \beta\alpha$$
$$\phi_4 = \beta\beta$$

Since the spin angular momentum operators are proportional to their component magnetizations, the x-y magnetization (from equation 2-4) may be written as

$$I_x + i\, I_y = I^+ \qquad \ldots. \qquad (2\text{-}8)$$

where I^+ is the raising operator. From equation (A-5) the average value of the x-y magnetization is:

$$\langle I^+ \rangle = \mathrm{Tr}(I^+ \rho) \tag{2-9}$$

Using the basis (2-7) the matrix for I^+ is

$$I^+ = \begin{bmatrix} 0 & 1 & 1 & 0 \\ 0 & 0 & 0 & 1 \\ 0 & 0 & 0 & 1 \\ 0 & 0 & 0 & 0 \end{bmatrix} \tag{2-10}$$

Therefore from (2-9) and (2-10) is obtained

$$\langle I^+ \rangle = \rho_{21} + \rho_{31} + \rho_{42} + \rho_{43} \tag{2-11}$$

The density matrix elements in (2-11) are calculated by solving the equation of motion (A-6) which has been modified as follows to account for exchange and relaxation:

$$\frac{d\rho}{dt} = i\left[\rho, \mathcal{H}\right]_+ \left(\frac{d\rho}{dt}\right)_{\text{exch}} + \left(\frac{d\rho}{dt}\right)_{\text{relax}} \tag{2-12}$$

The constant $\hbar$ has been omitted in the above equation so that the Hamiltonian is now expressed in units of radians/sec.

The matrix form of equation (2-12) is easily calculated (the matrices being given in appendix II). Then assuming unsaturated, steady-state conditions the left-hand side of (2-12) may be set equal to zero, which results in a system of linear algebraic equations from which the matrix elements of (2-11) may be determined. Only the imaginary part of (2-11) which represents the absorption signal detected by the spectrometer, is required

for the final solution. It can be shown (20) that this solution is

$$\mathrm{Im}\langle I^{+}\rangle = C\,\frac{\frac{\delta^2}{\tau}}{\Delta^4 - 2J\Delta^3 + \Delta^2\left(\frac{4}{\tau^2} - \frac{\delta^2}{2} + J^2\right) + \frac{\Delta\delta^2 J}{2} + \frac{\delta^4}{16}} + C\,\frac{\frac{\delta^2}{\tau}}{\Delta^4 + 2J\Delta^3 + \Delta^2\left(\frac{4}{\tau^2} - \frac{\delta^2}{2} + J^2\right) - \frac{\Delta\delta^2 J}{2} + \frac{\delta^4}{16}} \qquad (2\text{-}13)$$

Equation (2-13) defines the general line-shape function for an exchanging AB system. The relaxation terms have been neglected for simplification, so the expression is valid only in the intermediate exchange region where relaxation represents only a small contribution to the total linewidth. Furthermore the units are in radian/sec.

A simple explanation of how the general line-shape equation is utilized in calculating AB spectra as a function of lifetime will now be given. First of all, the chemical shift δ and coupling constant J are determined from the very slow exchange spectrum. Using these values and a particular lifetime, a plot of the right-hand side of expression (2-13) versus Δ is made. The result is an NMR absorption spectrum. A series of such spectra may be calculated for a given range of lifetimes. Computer programs are indispensable for calculating spectra in this way.

C. Determination of Rate Constants and Activation Parameters

For the equal population two-site exchange problem the mean lifetime τ is simply the inverse of the rate constant k. Probably the best way to obtain rate constants as functions of temperature is to compare visually, computer-calculated plots with the experimental spectra. This method gives the lifetimes or rate constants directly. With the wide-spread availability of computers the approximations derived from the early GMS theory have become more or less obsolete.

The activation energy, E_A, for the rate process may be determined from the Arrhenius equation:

$$k = A\, e^{-E_A/RT} \qquad \ldots \qquad (2\text{-}14)$$

where A is the frequency factor. If the rates are determined over a series of temperatures, a plot of log k versus 1/T should yield a straight line whose slope and intercept are proportional to E_A and log A respectively. This method implies that E_A and log A are independent of temperature which is a good approximation if the temperature range is small enough.

From the Eyring equation (27)

$$k = \frac{\kappa k_B T}{h}\, e^{-\Delta G^{\neq}/RT} \qquad \ldots\ldots \qquad (2\text{-}15)$$

where κ is the transmission coefficient, k_B is Boltzmann's constant and h is Planck's constant, the free energy of activation $\Delta G^{\neq}$ may be calculated at a given temperature.

Substitution of the thermodynamic equation

$$\Delta G^{\neq} = \Delta H^{\neq} - T\Delta S^{\neq} \quad \ldots\ldots \quad (2\text{-}16)$$

into (2-15) gives

$$k = \frac{\kappa k_B T}{h} \; e^{-\Delta H^{\neq}/RT} \; e^{\Delta S^{\neq}/R} \quad (2\text{-}17)$$

It can be shown that (27)

$$\Delta H^{\neq} = E_A - RT \quad \ldots \quad (2\text{-}18)$$

Substitution of (2-18) into (2-17) and comparison of the result with (2-14) shows that

$$\Delta S^{\neq} = 2.303R \left[\log\left(\frac{hA}{\kappa k_B T}\right) - 1 \right] \quad \ldots \quad (2\text{-}19).$$

Thus the enthalpy, $\Delta H^{\neq}$, and entropy of activation, $\Delta S^{\neq}$, may be calculated from the Arrhenius plots and from equations (2-18) and (2-19) respectively.

However, according to Binsch (4), the above approach is not consistent since E_A and log A are assumed to be temperature-independent while $\Delta H^{\neq}$ and $\Delta S^{\neq}$ are dependent on the temperature. He suggests that a more logical approach would be to obtain $\Delta H^{\neq}$ and $\Delta S^{\neq}$ in the following way: Taking the log of both sides of (2-17) yields

$$\log\left(\frac{k}{T}\right) = -\frac{\Delta H^{\neq}}{2.303R}\left(\frac{1}{T}\right) + \log\left[\frac{\kappa K_B}{h} + \frac{\Delta S^{\neq}}{2.303R}\right] \quad (2\text{-}20)$$

Now a plot of log (k/T) versus 1/T should give a straight line whose slope and intercept are proportional to $\Delta H^{\neq}$ and $\Delta S^{\neq}$ respectively. In this way the enthalpy and entropy of activation are assumed to be independent of temperature.

D. Sources of Error

Probably the greatest drawback in NMR rate studies is the magnitude of the systematic errors inherent in the method. The sources of these errors as they apply to GMS theory have been discussed in a recent paper (28). It was found that in many cases the classical equation was oversimplified or one of the approximate formulae was used in a case where it did not apply and thus a serious systematic error was introduced.

Many of these systematic errors may be eliminated by using the quantum mechanical line-shape theory. However, even this method suffers from the fact that the temperature range over which significant spectral changes occur is rather small and that the spectral sensitivity is not uniformly distributed over this range. Since changes in line-shape occur much more rapidly in the intermediate region near the coalescence temperature than at the extremes, the data in this region will be more reliable. Reeves (2) suggests that the range of lifetimes where detectable linewidth changes occur is given by

$$\frac{16}{\delta\nu_{AB}} > \tau > \frac{0.0016}{\delta\nu_{AB}}$$

At the limits of fast and slow exchange the main contributions to the linewidths arise from the inhomogeneity of the external magnetic field and the relaxation processes. In fact the following equation has been given (29) to represent this fact:

$$\frac{1}{T_2} = \frac{1}{T_2^o} + \frac{1}{T_2'}$$

where $1/T_2$ is a measure of the observed linewidth at half-height of the resonance peak and T_2 is called the effective relaxation

time. T_2^o is the transverse relaxation time and $1/T_2'$ is a measure of the inhomogeneity and other instrumental contributions to the linewidth. A properly chosen value of the effective T_2 is required for the line-shape expressions. It is often deduced from the linewidths of a peak at very fast or very slow exchange or from some standard peak due to a non-exchanging proton. Equation (2-6) is then used to obtain T_2 from the linewidth. However, such a value is not very reliable since T_2^o is different for nuclei with different environments and varies with temperature (17). Furthermore the inhomogeneity contribution is extremely sensitive and difficult to keep constant. The error due to an improperly chosen T_2 will be small in the intermediate exchange region and large at the extremes, but the total effect will be an observable error in the slope of the Arrhenius plot.

Another systematic error will be introduced if the relative chemical shift of the two exchanging protons is temperature-dependent. Since this shift can usually be measured only at the slow exchange limit, it has been considered constant in many calculations. If in fact there is a temperature variation, the calculated rates will be wrong especially in the coalescence region (17) and a significant systematic error will result in the activation energy. One way to correct for this error is to measure the relative shift at several slow exchange temperatures and to extrapolate into the fast exchange region. Various workers have applied corrections of this kind (30-32).

The effect of the preceding errors in the activation parameters increases in the following order: $\Delta G^{\neq} < \Delta H^{\neq} < \Delta S^{\neq}$. These differences follow directly from the equations used to calculate the parameters (29).

In addition to the systematic errors, numerous experimental errors may arise from instrumental difficulties. These include temperature variations, field inhomogeneity and saturation effects (28). A knowledge of the accurate sample temperature is imperative in rate studies. Fluctuations may result from variations in heater current or flow rate of the gas. There will also be temperature gradients within the probe which become more serious the farther away from normal magnet temperature the measurement is being performed. However, if the temperature is determined with the standard methanol or ethylene glycol samples immediately before or after a run is made, the uncertainty in the relative temperature should be less than $\pm 1^{\circ}C$.

Serious distortions of the resonance peaks will result from an inhomogeneous magnetic field, the use of excessive filtering and from saturation effects. Inhomogeneity will cause excessive broadening which will have serious effects in the slow and fast exchange regions. This effect is especially noticeable when the temperature is suddenly changed and for this reason the resolution should always be checked for each temperature run. Saturation and too much filtering will also cause distorted line-shapes

and so must be carefully avoided. If there precautions are taken the observed resonance peaks should approximate true Lorentzians as implicitly assumed by the underlying theory.

CHAPTER III

Nature of the Problem

At -40°C the proton magnetic resonance of α,α,2,4,6-pentachlorotoluene consists of an ABX spectrum, the AB part due to the ring protons and the X part due to the methine proton. As the compound is heated the AB part broadens and finally coalesces into a single peak at 20°C. Upon further heating this peak begins to sharpen until at 70°C an A_2X spectrum is observed (a doublet for the ring protons and a triplet for the methine proton). From these observations it is clear that a rate process involving hindered rotation of the dichloromethyl group of the compound must be taking place.

The purpose of this investigation is to determine rate constants and activation parameters for this hindered rotation by matching experimental and computer-calculated spectra. An attempt to explain the mechanism for this rate process will also be made.

CHAPTER IV

Experimental

A. Compounds

The compound α,α,2,4,6-pentachlorotoluene (pentachlorotoluene) was prepared in the following three steps:

1. Ring chlorination of m-toluidine

   The method of White and Adams (33) was followed. m-toluidine was first acetylated with acetic anhydride and the product chlorinated by passing a continuous stream of chlorine into the mixture for six to eight hours. The acetyl derivative was converted to the free amine, 2,4,6-trichloro-3-amino toluene, by addition of sulfuric acid and steam distillation.

2. Deamination

   The method used was similar to that of Chattaway and Evans (34). A solution of sodium nitrite in ethanol was added to an ethanolic solution of the trichloro-m-toluidine prepared above and the mixture was agitated. After being allowed to stand for several hours the mixture was steam distilled. The product 2,4,6-trichlorotoluene crystallized out in the collection flask. Its purity was checked by its melting point (25 - 27°C) and by the appearance of the NMR spectrum of a 10 mole% solution of the compound in carbon disulfide.

3. Chlorination of the sidechain

   The trichloro derivative from the preceding step was chlorinated under UV light for three hours at which time its

weight indicated that it had been dichlorinated. The product α,α,2,4,6-pentachlorotoluene was distilled three times, the distillate being collected, and its purity deduced from the appearance of its NMR spectrum. There was one small impurity peak in the spectrum which, from subsequent work in this laboratory, has been shown to be due to α,α,α,2,4,6-hexachlorotoluene. Its presence in no way affected the rate study; in fact this peak was used to obtain an estimate of the effective T_2.

The other chemicals used were toluene-d_8, methylcyclohexane (MeC_6H_{11}), carbon disulfide (CS_2), acetone, dimethyl formamide (DMF), cyclopentane (C_5H_{10}) and tetramethylsilane (TMS). They were obtained from the following chemical companies and used without further purification: Aldrich Chemical Co. Inc., Nuclear Magnetic Resonance Specialties, Matheson Coleman and Bell, and Chem Service.

B. Proton Magnetic Resonance Measurements

All proton magnetic resonance (PMR) spectra were measured on a Varian DA-60 I Spectrometer operated in the frequency sweep mode and locked to internal TMS. Calibrations were carried out by period averaging techniques, all spectra being recorded at least four times. The shifts were reported with an accuracy of ± 0.005 ppm and the errors in the coupling constants were standard deviations from the mean. Approximately 15 mole % solutions of pentachlorotoluene in toluene-d_8, Me C_6H_{11}, CS_2, acetone and DMF were prepared with about 1 mole % of C_5H_{10} added to each one. Each solution was degassed using the freeze-pump-thaw technique.

The temperature studies were then carried out as follows. After each sample had been heated in a boiling water bath to see whether the tubes could withstand the added pressure, PMR spectra were recorded at approximately 10° intervals. The spectrometer was equipped with a Varian V-4343 variable temperature controller. All temperatures were determined immediately after each calibration using an ethylene glycol or methanol standard and the graph of internal shift versus temperature prepared by Varian. Optimum resolution at each temperature was checked by the appearance of the methine proton peak and the C_5H_{10} standard peak. All spectra were recorded with a sweep rate of 0.02 H_z/sec.

CHAPTER V

Results

All the chemical shifts in this study are given in PPM to low field of internal TMS and all coupling constants and linewidths at half-height are reported in H_z.

The proton chemical shifts and coupling constants for the 10 mole % solution of 2,4,6-trichlorotoluene were determined from its spectrum by simple first order rules. The results were as follows:

ν_A = 7.169 ± 0.005 ppm

ν_X = 2.369 ± 0.005 ppm

J_{AX} = 0.48 ± 0.02 H_z

where A refers to the ring protons and X to the methyl protons.

Of the temperature studies carried out, rates were determined only for the toluene-d_8 and MeC_6H_{11} solutions. The low temperature spectrum of the CS_2 solution was an ABC and rates could not be determined with the present computer program. The solute came out of solution in the acetone and DMF solvents before the slow exchange temperature could be reached.

Some of the PMR spectra at various temperatures are shown in figures 1,2,3,5 and 6. Proton assignments were made for the ABX spectra obtained at the lowest temperatures (figures 1 and 2) with reference to the following conformation of pentachlorotoluene (later shown to be the ground state):

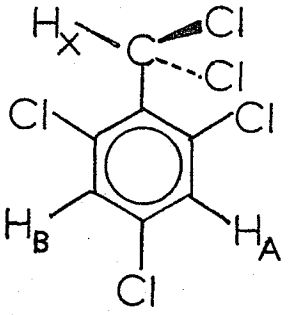

The doublet to lowest field was assigned to H_X. Its low shielding was due to the magnetic anisotropy of the ring and hydrogen-bonding with the ortho-chlorine atom (35). Furthermore its long-range coupling to only one ring proton was consistent with the zig-zag rule (36). H_A was less shielded than H_B because of the sidechain chlorine atoms and therefore its resonance was to lower field. The slight broadening of the H_B resonance lines seemed to indicate a small coupling (<0.1 H_Z) to H_X. Finally the greater chemical shift difference between the H_A and H_B resonance peaks in the toluene-d_8 solution was due to an aromatic solvent induced shift (ASIS).

A complete list of the chemical shifts and linewidths at half-height of the resonance peaks in the spectra of the toluene-d_8 and MeC_6H_{11} solutions is given in Tables I - ^{VI}. The widths at half-height of the C_5H_{10} and impurity peaks are also shown.

FIGURE-I

The PMR spectrum of a 15 mole % solution of pentachlorotoluene in toluene-d_8 at -39.7°C.

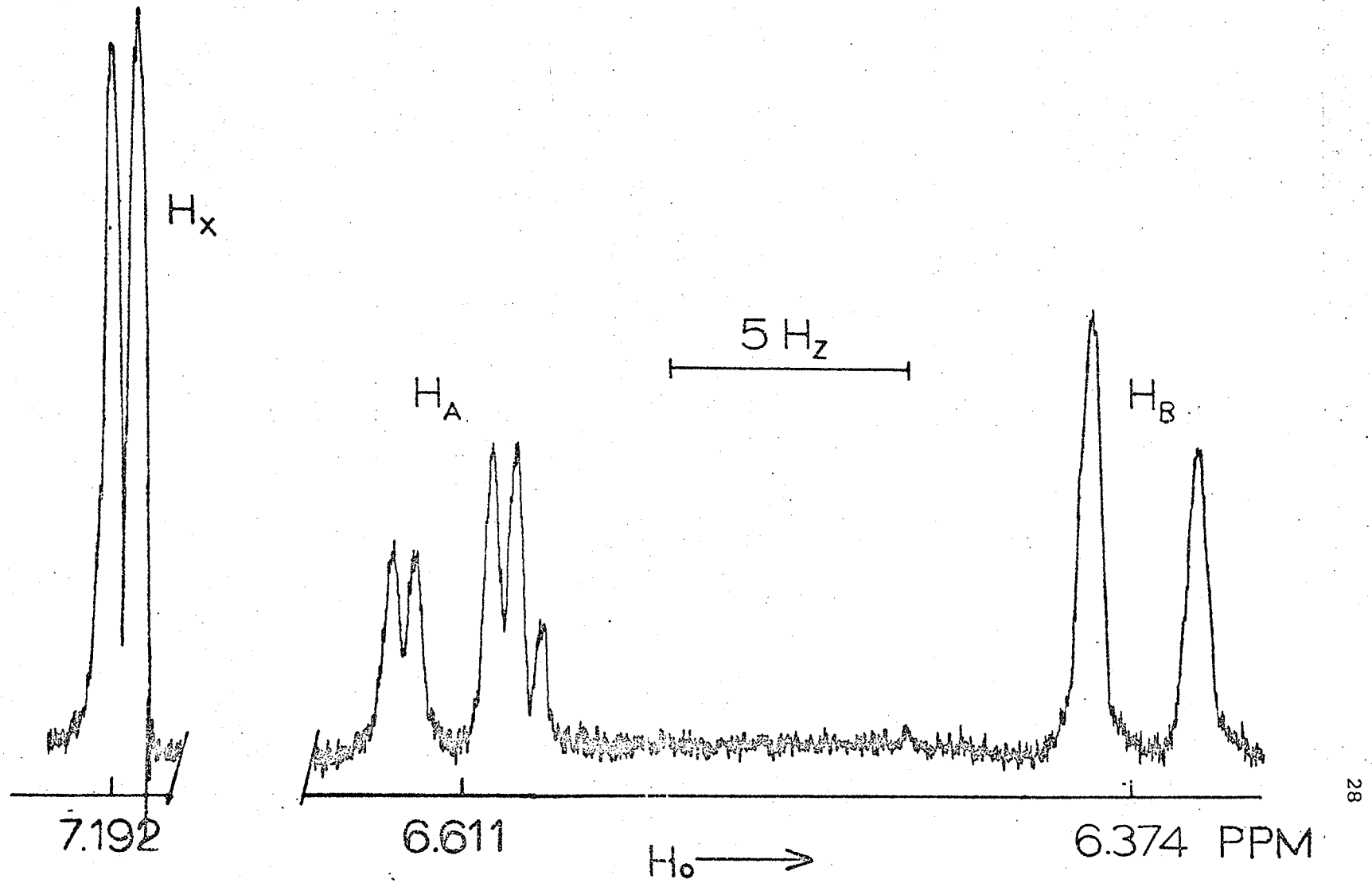
H_X
5 Hz
H_A
H_B
7.192
6.611
6.374 PPM
H_o

FIGURE 2

The PMR spectrum of a 15 mole % solution of pentachlorotoluene in MeC_6H_{11} at -37.0°C.

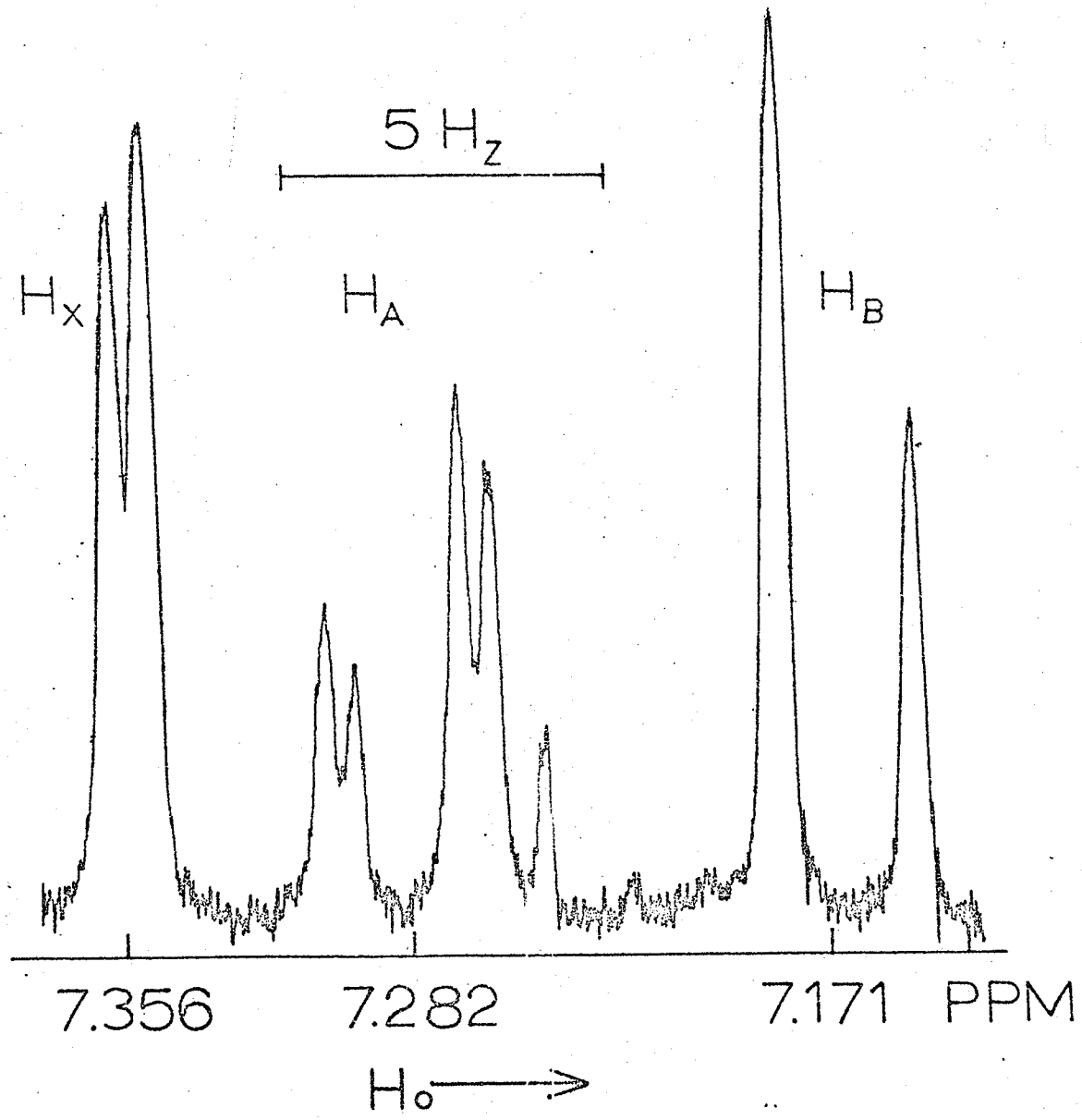
5 Hz
Hx
HA
HB
7.356
7.282
7.171 PPM
Ho

FIGURE 3

The PMR spectra of 15 mole % solutions of pentachlorotoluene in (a) MeC_6H_{11} at 71.9°C and (b) toluene-d_8 at 72.6°C.

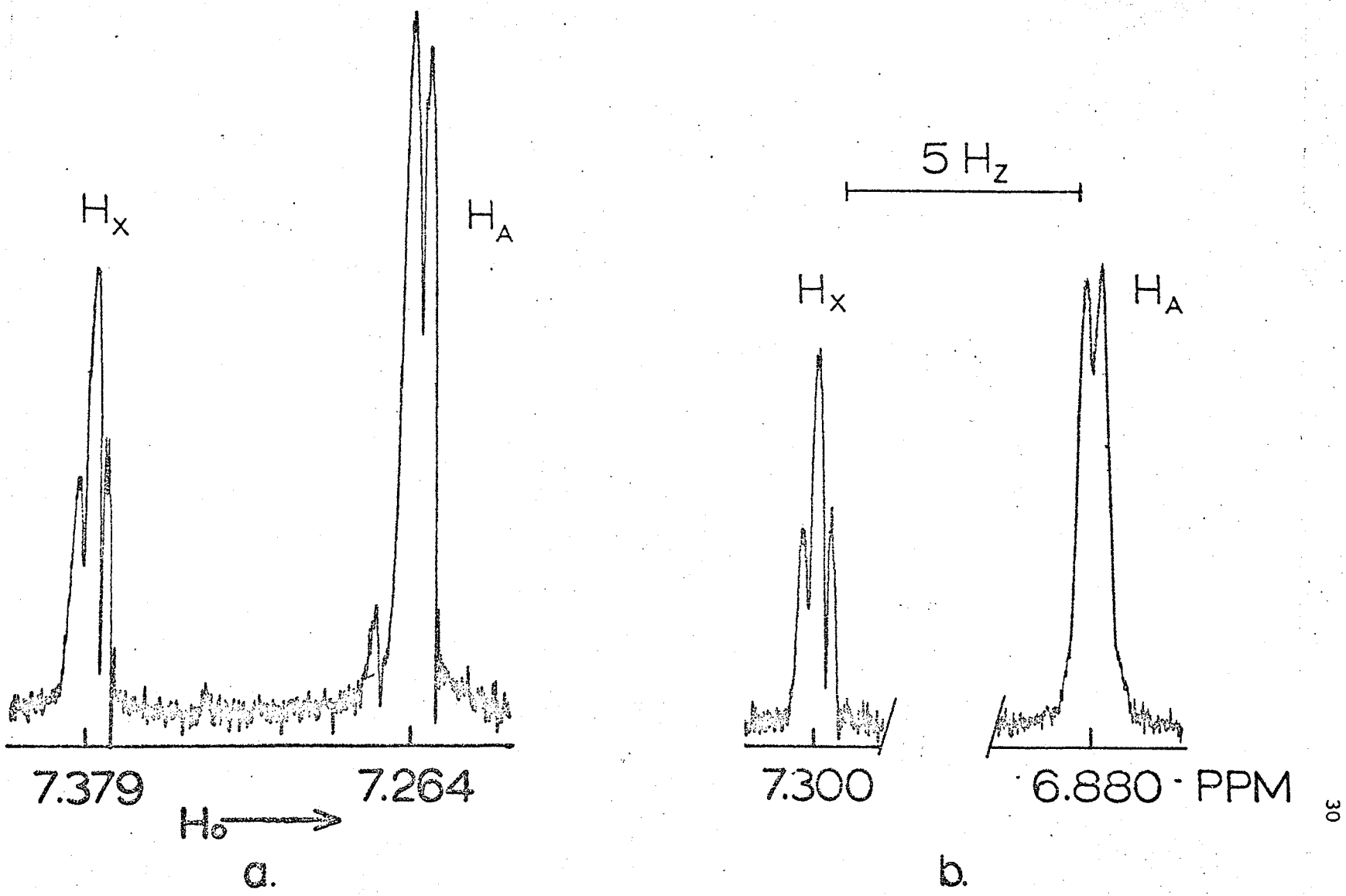
5 Hz
Hx
HA
Hx
HA
7.379
7.264
Ho
7.300
6.880 · PPM
a.
b.

TABLE - I

Chemical shifts and linewidths of the H_A resonance peaks below coalescence for the Toluene-d_8 solution.

TEMP. (^oC)	CHEMICAL SHIFTS (PPM) AND LINEWIDTHS (H_z)			
-39.7	6.634*	6.625	6.598	6.590
	0.46	0.40	0.49	0.40
-24.9	6.699	6.691	6.663	6.655
	0.91	- **	0.93	-
-8.8	6.761	-	6.722	-
	1.11	-	1.09	-
-3.2	6.783	-	6.747	-
	3.93	-	1.47	-
2.7	6.798	-	6.769	-
	4.56	-	-	-
10.0	6.781	-	-	-
	4.22	-	-	-

* In this and subsequent tables the shifts are given in the first row and their respective linewidths at half-height in the second row opposite a given temperature.

** A dash means that the resonance peaks have begun to overlap.

TABLE - II

Chemical shifts and linewidths of the H_B and H_X resonance peaks below coalescence for the toluene-d_8 solution.

TEMP. (°C)	CHEMICAL SHIFTS (PPM) AND LINEWIDTHS (H_z) H_B		H_X			C_5H_{10}	IMP.**
-39.7	6.391	6.355	7.197	7.188			
	0.50	0.49	*			0.39	0.28
-24.9	6.466	6.430	7.216	7.206			
	0.55	0.54				0.42	0.32
- 8.8	6.542	6.507	7.237	7.231	7.226		
	0.62	0.70				0.29	0.21
- 3.2	6.571	6,536	7.244	7.238	7.233		
	1.09	3.77				0.32	0.20
2.7	6.595	6.562	7.249	7.243	7.238		
	4.56	-				0.37	0.20
10.0	6.610	-	7.253	7.248	7.242		
	-	-				0.24	0.20

* A blank in this and subsequent tables means that no data are required or is available for the given space.

** This represents the impurity peak.

TABLE - III

Chemical shifts and linewidths of the H_A and H_X resonance peaks above coalescence for the toluene-d_8 solution.

TEMP. (°C)	CHEMICAL SHIFTS (PPM) AND LINEWIDTHS (H_Z) H_A		H_X			C_5H_{10}	IMP.
27.2	6.760		7.273	7.267	7.262		
	5.82					0.33	0.28
30.3	6.767		7.276	7.270	7.265		
	4.43					0.29	0.29
34.2	6.777		7.277	7.272	7.267		
	3.64					0.32	0.20
49.9	6.824		7.290	7.284	7.279		
	1.14					0.34	0.24
58.8	6.844		7.298	7.292	7.288		
	0.83					0.30	
72.6	6.882	6.878	7.305	7.300	7.295		
	0.70	--				0.36	

TABLE - IV

Chemical shifts and linewidths of the H_A resonance peaks below coalescence for the MeC_6H_{11} solution.

TEMP. (°C)	CHEMICAL SHIFTS (PPM) AND LINEWIDTHS (H_z)			
-37.0	7.306	7.298	7.270	7.262
	0.41	0.83	0.42	0.41
-17.0	7.316	7.309	7.280	7.272
	0.94	-	0.92	-
- 8.5		-	7.287	7.279
	1.08	-	0.99	-
- 0.8	7.321	-	7.287	-
	1.39	-	-	-
7.3	7.287	-	-	-
	6.45	-	-	-
14.4	7.268	-	-	-
	5.87	-	-	-

TABLE - V

Chemical shifts and linewidths of the H_B and H_X resonance peaks below coalescence for the MeC_6H_{11} solution

TEMP. (°C)	CHEMICAL SHIFTS (PPM) AND LINEWIDTHS (H_z) H_B		H_X			C_5H_{10}	IMP.
-37.0	7.186	7.151	7.361	7.352			
	0.45	0.37				0.46	0.26
-17.0	7.197	7.161	7.366	7.356			
	0.45	0.43				0.32	0.20
- 8.5	7.205	7.170	7.369	7.364	7.359		
	0.51	0.62				0.30	0.18
- 0.8	7.226	7.174	7.372	7.366	7.360		
	0.91	-				0.27	0.18
7.3	7.218	-	7.373	7.368	7.362		
	-	-				0.28	0.18
14.4	7.232	-	7.374	7.369	7.364		
	-	-				0.24	0.18

TABLE - VI

Chemical shifts and linewidths of the H_A and H_X resonance peaks above coalescence for the MeC_6H_{11} solution

TEMP. (°C)	CHEMICAL SHIFTS (PPM) AND LINEWIDTHS (H_z) H_A		H_X			C_5H_{10}	IMP.
23.5	7.256		7.376	7.370	7.365		
	3.35					0.31	0.20
30.7	7.256		7.378	7.372	7.367		
	1.70					0.30	0.20
43.5	7.260		7.380	7.374	7.370		
	0.94					0.28	0.18
52.8	7.263	7.258	7.381	7.375	7.370		
	0.80	-				0.31	0.18
71.9	7.266	7.261	7.384	7.378	7.374		
	0.75	-				0.32	0.21

The results of standard ABX analyses (7) of the lowest temperature spectra (figures 1 and 2) as well as simple first order analyses of the highest temperature A_2X spectra (figure 3) of the two solutions are given in Table VII.

TABLE - VII

Proton chemical shifts and coupling constants for the ABX and A_2X spectra of the toluene-d_8 and MeC_6H_{11} solutions

	TOLUENE-d_8	MeC_6H_{11}
ABX		
ν_A (ppm)	6.611 ± 0.005	7.282
ν_B	6.374	7.171
ν_X	7.192	7.356
J_{AB} (H_z)	2.14 ± 0.04	2.14 ± 0.04
J_{AX}	0.52 ± 0.02	0.50 ± 0.02
J_{BX}	0.01	0.01
A_2X		
ν_A (ppm)	6.880	7.264
ν_X	7.300	7.379
J_{AX} (Hz)	0.30 ± 0.02	0.33 ± 0.02

CHAPTER VI

Discussion of Results

A. Treatment of Data

1. Determination of Rate Constants

The rate constants were obtained by matching the linewidths at half-height of the resonance peaks of the experimental spectra as closely as possible to the calculated widths. These calculated widths were obtained from the computer program for ABX exchange (26) which gave widths at half-height for the peaks in the AB part of the spectrum as a function of lifetime. The input parameters were $\delta\nu_{AB}$, J_{AB}, J_{AX}, J_{BX} and T_2.

The two main problems associated with this rate determination were:

(1) A method had to be found for determining an effective T_2 value.

(2) A method had to be found to account for the variation of $\delta\nu_{AB}$ with temperature in the toluene-d_8 solution.

How these two problems were dealt with will now be discussed.

(1) Effective Relaxation Time Problem

The following three methods were employed to obtain an effective T_2 for use in the ABX exchange program:

a. T_2 was calculated at each temperature from the linewidth at half-height of the C_5H_{10} peak using the formula

$$\Delta\nu_{\frac{1}{2}} = \frac{1}{T_2}$$

In this way values ranging from 2.4 to 4.2 sec. were obtained.

b. The C_5H_{10} peak widths were used with the "correct" equation (2-6),

$$\Delta\nu_{\frac{1}{2}} = \frac{1}{\pi T_2}$$

This time smaller values, ranging from 0.8 to 1.3 sec. were obtained.

c. The linewidths of the impurity peak were used in equation (2-6). Since these linewidths varied very little with temperature, an average T_2 was calculated for each solution. These values were 1.38 sec. for the toluene-d_8 solution and 1.59 sec. for the MeC_6H_{11} solution.

Three sets of rate constants for each solution were calculated using the above methods. A linear relationship was assumed between log k and 1/T and least squares analyses were carried out on the data. The activation energies were calculated by multiplying the slopes by 2.303R. All the data along with the results of the least squares analyses are collected in Tables VIII and IX.

TABLE VIIIa

Rate constants for the toluene-d_8 solution using the three methods for obtaining T_2.

TEMP (°C)	$\frac{1}{T} \times 10^3$ ($^oK^{-1}$)	METHOD a		METHOD b		METHOD c	
		τ (sec)	log k	τ(sec.)	log k	τ (sec)	log k
72.6	2.892	0.00115	2.939	-	-	0.00033	3.481
58.8	3.012	0.00185	2.733	-	-	0.00105	2.979
49.9	3.095	0.00295	2.530	0.00168	2.77_5	0.00230	2.638
34.2	3.253	0.0105	1.979	0.00980	2.009	0.0101	1.996
30.3	3.295	0.0126	1.900	0.0120	1.919	0.0122	1.914
27.2	3.329	0.0150	1.824	0.0154	1.812	0.0156	1.806
10.0	3.531	0.115	0.939	0.125	0.903	0.125	0.903
2.7	3.625	0.190	0.721	0.220	0.658	0.211	0.676
-3.2	3.704	0.318	0.498	0.375	0.426	0.366	0.437
-8.8	3.782	0.645	0.190	0.950	0.022	0.865	0.063
-24.9	4.027	-	-	3.50	-0.544	-	-

TABLE VIIIb

Results of least squares analyses of data from Table VIII-a

METHOD	SLOPE ($^oK \times 10^3$)	INTERCEPT	δ_y^*	$\delta_m \times 10^3$	δ_b	E_A (kcal/mole)
a.	-3.23	12.4	0.086	0.09	0.3	14.8
b.	-3.61	13.8	0.107	0.13	0.4	13.8
c.	-3.78	14.4	0.057	0.06	0.2	17.3

* δ_y, δ_m and δ_b represent the standard errors in log k, the slope and the intercept respectively.

TABLE IX-a

Rate constants for the MeC_6H_{11} solution using the three methods for obtaining T_2

TEMP (°C)	$\frac{1}{T} \times 10^3$ (°K^{-1})	METHOD a		METHOD b		METHOD c	
		τ (sec)	log k	τ (sec)	log k	τ (sec)	log k
52.8	3.067	0.00520	2.284	-	-	0.00780	2.108
43.5	3.158	0.00790	2.102	0.00560	2.252	0.0105	1.979
30.7	3.291	0.0196	1.708	0.0177	1.749	0.0214	1.670
23.5	3.370	0.0387	1.412	0.0373	1.428	0.0397	1.401
14.4	3.477	0.0671	1.173	0.0665	1.177	0.0690	1.161
7.3	3.565	0.0840	1.076	0.0780	1.098	0.0891	1.050
-0.8	3.671	0.0333	0.478	0.370	0.432	0.288	0.541
-8.5	3.778	1.01	-0.004	1.40	-0.146	0.815	0.089
-17.0	3.903	1.72	-0.236	-	-	1.25	-0.097

TABLE IX-b

Results of least squares analyses of data from Table IX-a

METHOD	SLOPE (°K x 10^3)	INTERCEPT	δ_y	$\delta_m \times 10^3$	δ_b	E_A (kcal/mole)
a.	-2.81	10.8	0.075	0.09	0.3	12.8
b.	-3.75	14.2	0.134	0.20	0.7	17.2
c.	-3.12	12.0	0.108	0.14	0.5	14.3

The blanks in the preceding tables represent points which were disregarded in the least squares analyses because a very poor linewidth fit was obtained. These points also deviated by a large amount from the straight line plots. Weighting the points at the ends of the plots less than those in the middle was also tried, since the intermediate points are more reliable. However, the differences involved lay within the experimental errors, so all points used were taken with equal weight.

The three methods used for obtaining T_2 will now be discussed in the light of the preceding results. With method (a), when experimental and calculated widths were matched at the high temperature limit, no splitting was observed in the calculated spectra. For the low temperature spectra, the calculated peaks were not split as much as the experimental ones. The corresponding Arrhenius plots deviated greatly from the straight line at these extremes. When method (b) was used, the calculated, fast exchange linewidth approached a limiting value which was larger than that of the experimental peak. A greater deviation from the straight line than that obtained from method (a) was observed. Finally method (c) yielded results similar to the first one; however a better straight line was obtained. In all cases the fit in the intermediate exchange region was reasonably good.

In the present study it was finally decided to use method (c) in determining the activation parameters for the following reasons:

1. The impurity peak was due to a compound closely related to pentachlorotoluene.
2. The width of the peak varied very little with temperature.
3. A good fit between experimental and calculated spectra was obtained in the intermediate exchange region.
4. The best straight line plot was obtained using this method.

From this discussion it should be noted that an error in T_2 introduces a large systematic error into the activation parameters. An estimate of this error was obtained by taking the difference between the largest and smallest activation energies and frequency factors obtained from the least squares analyses in the three methods (Tables VIII-b and IX-b). These results are listed below.

SOLVENT	PARAMETER	MAX UNCERTAINTY
Toluene-d_8	E_A	± 1.3 kcal/mole
	log A	± 1.0
MeC_6H_{11}	E_A	± 2.2 kcal/mole
	log A	± 1.7

Various methods used by other workers to determine an effective transverse relaxation time may be found in the following references (31,37-40).

(2) Variable Shift problem

At -40°C the chemical shift difference between the ring proton resonance peaks of pentachlorotoluene was much larger in the toluene-d_8 than in the MeC_6H_{11} solution. Furthermore there was a much greater high field shift of these peaks in the toluene-d_8 solution. From this evidence it was clear that an aromatic solvent induced shift (ASIS) effect was being observed. Essentially this effect is concerned with the large magnetic anisotropy of aromatic rings. Because of this anisotropy, protons of a compound, dissolved in an aromatic solvent, which are situated above the ring and near the six-fold axis experience large upfield shifts relative to those of the same compound in an "inert" solvent such as cyclohexane. An increase in temperature causes a decrease in the ASIS and hence downfield shifts of the proton resonance peaks. Good reviews and discussions of the ASIS have been given (41, 42).

In the present study the relative shift of the ring proton resonance peaks of the toluene-d_8 solution decreased with increasing temperature because H_B was experiencing a larger ASIS than H_A. The probable reason for this larger effect is that it is easier for the aromatic ring of the solvent to lie directly over H_B because there is less steric hindrance in this position. In any case the relative shift as a function of temperature was estimated before coalescence by comparing the peak positions of the experimental spectra with those which were calculated by assuming a constant shift of 14.17Hz.

These results are listed in Table X-a. As can be seen from the plot of this data in figure 4 the relationship is linear over this temperature range. Therefore the relative shift at higher temperatures was estimated by extrapolation, these results being shown in Table X-b.

A new set of rate constants for the toluene-d_8 solution was determined using the new values of relative shift, $\delta\nu_{AB}$, which were just calculated. The effective relaxation time of 1.38 sec. was used. The new rate constants along with the least squares analysis are given in Table XI.

The new activation energy obtained when the shift variation was accounted for differed by 2.1 kcal/mole from that obtained by assuming a constant shift. The difference between this activation energy and that for the MeC_6H_{11} solution was within the standard error limits. Therefore it was concluded that this type of correction should be made and all subsequent activation parameters were calculated on this basis. Further discussion of this systematic error may be found in several papers (17,30,31).

TABLE - Xa

Variation in relative shift with temperature of the ring protons for the toluene-d_8 solution.

TEMP. (^oC)	$\delta\nu_{AB}$ (H_z)
-39.7	14.17
-24.9	13.54
- 8.8	12.99
- 3.2	12.62
2.7	12.48

TABLE - Xb

Variation in relative shift with temperature of the ring protons for the toluene-d_8 solution, estimated by extrapolation.

TEMP. (^oC)	$\delta\nu_{AB}$ (H_z)
10.0	12.17
27.2	11.48
30.3	11.35
34.2	11.20
49.9	10.57
58.8	10.21
72.6	9.65

FIGURE 4

A plot of the chemical shift difference $\delta\nu_{AB}$ between the ring proton resonance peaks of the toluene-d_8 solution versus temperature.

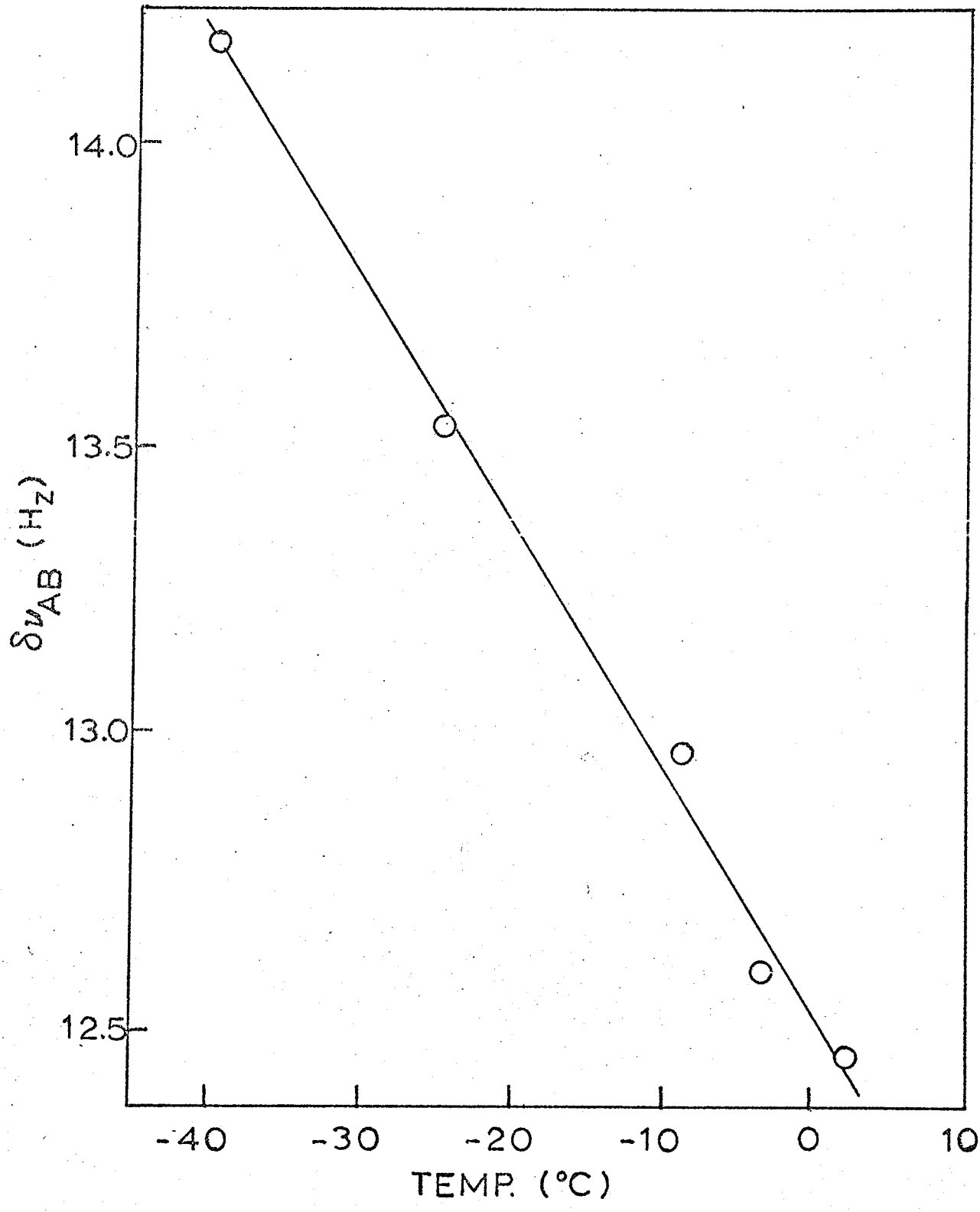
14.0
13.5
13.0
12.5
$\delta\nu_{AB}$ (Hz)
-40
-30
-20
-10
0
10
TEMP. (°C)

TABLE XI

Rate constants for the toluene-d_8 solution determined by using a T_2 of 1.38 sec. and by varying the relative shift

TEMP. (^oC)	$\frac{1}{T} \times 10^3$ ($^oK^{-1}$)	τ(sec.)	log k
72.6	2.892	0.00071	3.149
58.8	3.012	0.0020	2.699
49.9	3.095	0.00419	2.378
34.2	3.253	0.0157	1.804
30.3	3.295	0.0184	1.735
27.2	3.329	0.0227	1.644
10.0	3.531	0.116	0.937
2.7	3.625	0.214	0.670
-3.2	3.704	0.347	0.460
-8.8	3.782	0.777	0.110

Slope = 3.32×10^3 $^oK^{-1}$
Intercept = 12.7
δ_y = 0.052
δ_m = 0.05×10^3 $^oK^{-1}$
δ_b = 0.2
E_A = 15.2 kcal/mole

Several spectra of the toluene-d_8 and MeC_6H_{11} solutions at various temperatures are shown in figures 5 and 6 together with their corresponding calculated spectra which were plotted on the Calcomp plotter. Details may be found in reference (26). An effective T_2 of 1.38 sec. and a variable shift were used in the calculations for the toluene-d_8 solution and an effective T_2 of 1.59 sec. was used in those for the MeC_6H_{11} solution. The Arrhenius plots for the two solutions are shown in figures 7 and 8.

FIGURE 5

Experimental and calculated PMR spectra of the ring proton resonance peaks for the toluene-d_8 solution at various temperatures and corresponding lifetimes.

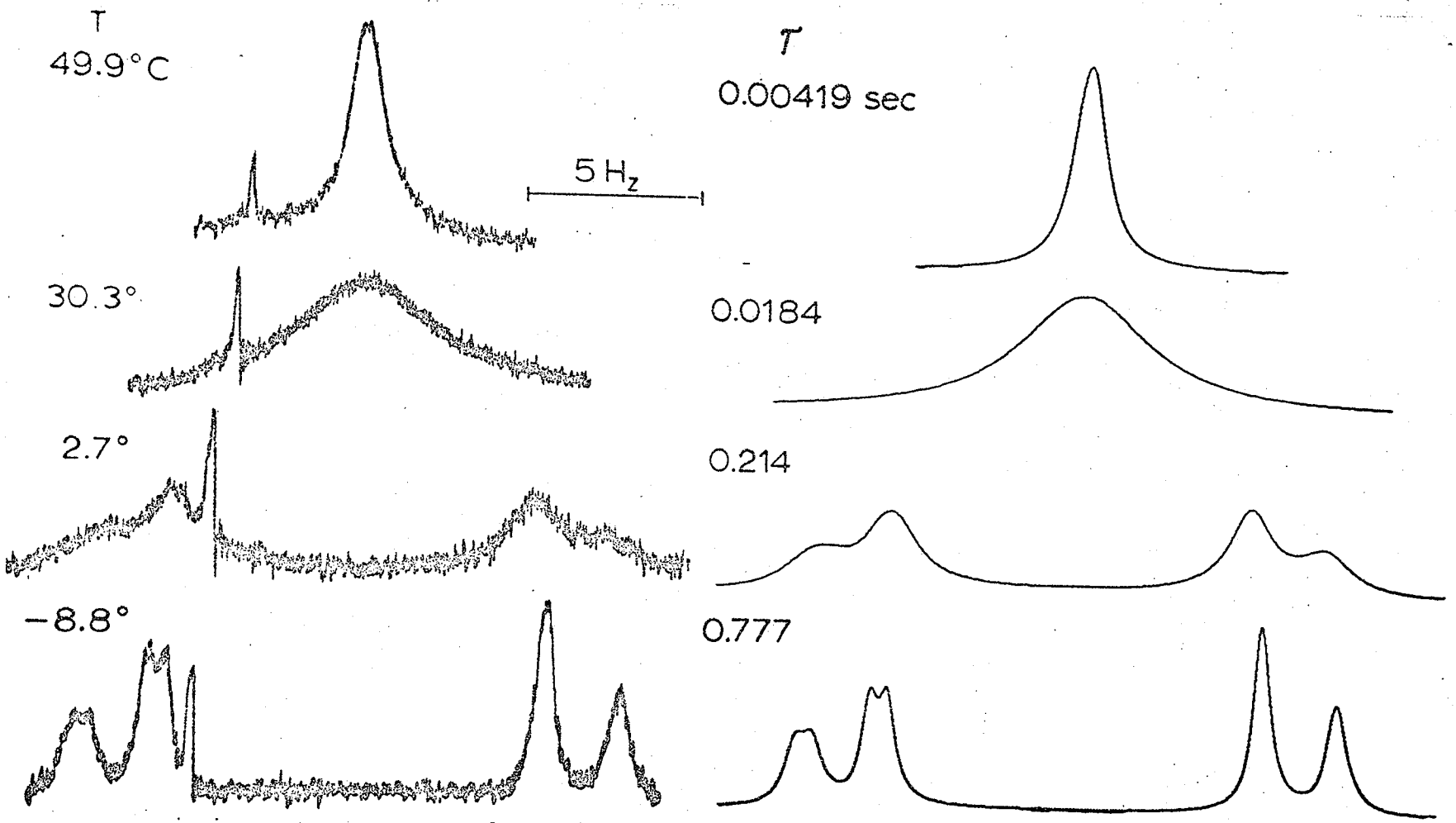
T
49.9°C
5 Hz
30.3°
2.7°
−8.8°
τ
0.00419 sec
0.0184
0.214
0.777

FIGURE 6

Experimental and calculated PMR spectra of the ring proton resonance peaks for the MeC_6H_{11} solution at various temperatures and corresponding lifetimes.

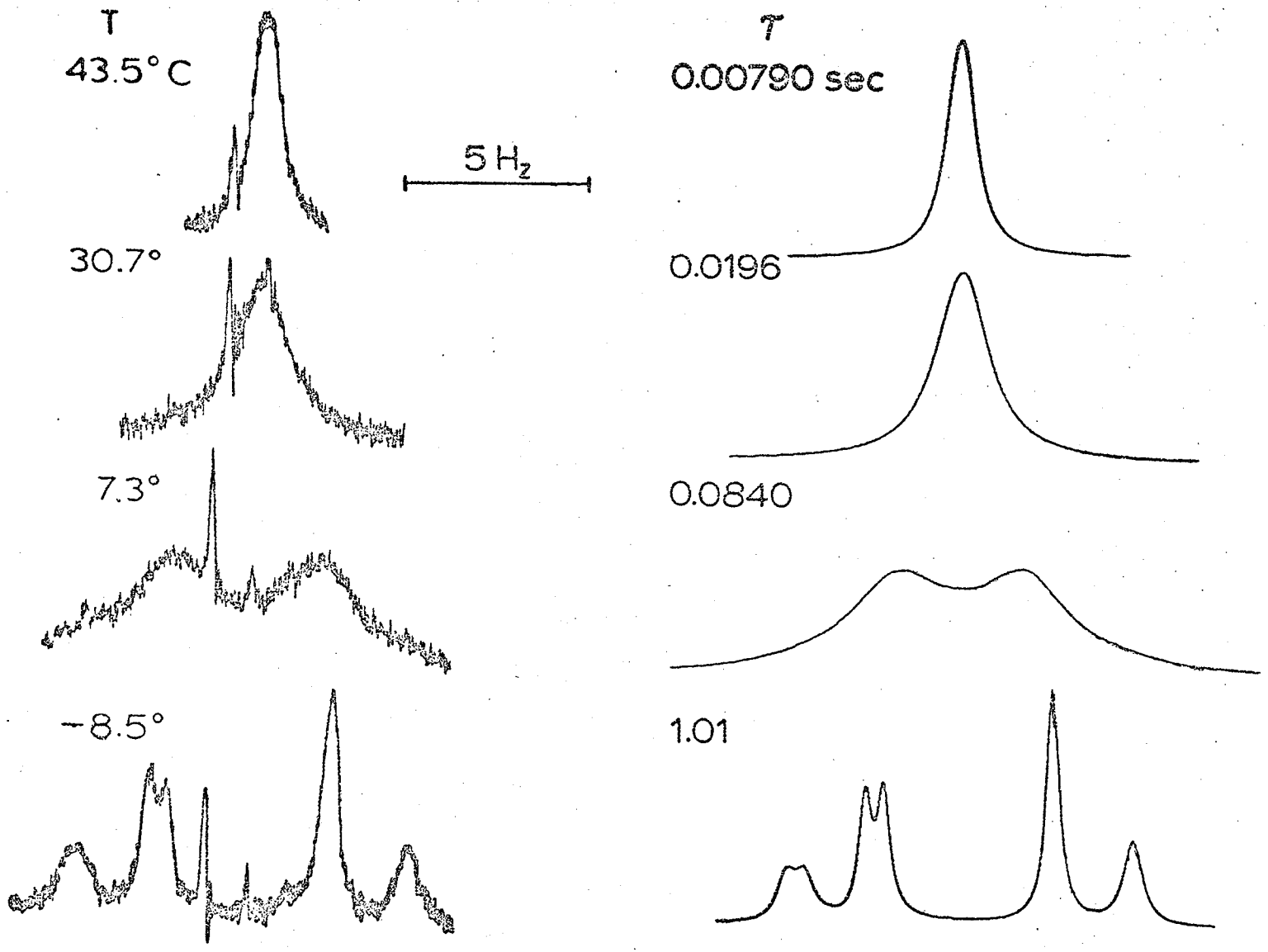
T
43.5° C
5 Hz
30.7°
7.3°
−8.5°
τ
0.00790 sec
0.0196
0.0840
1.01

FIGURE 7

A plot of log k versus $\frac{1}{T}$ for the toluene-d_8 solution.

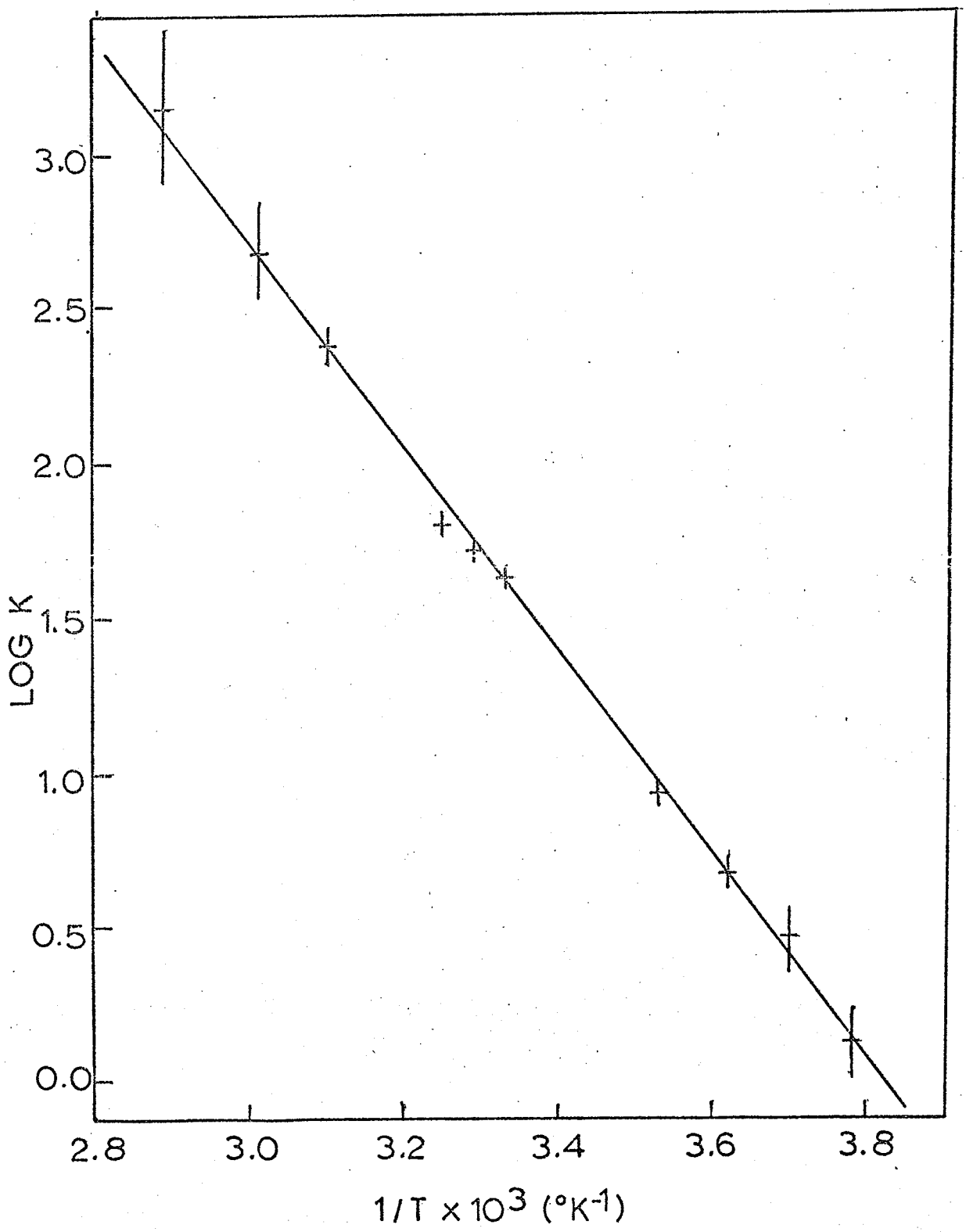
3.0
2.5
2.0
1.5
1.0
0.5
0.0
LOG K
2.8
3.0
3.2
3.4
3.6
3.8
1/T x 10³ (°K⁻¹)

FIGURE 8

A plot of log k versus $\frac{1}{T}$ for the MeC_6H_{11} solution.

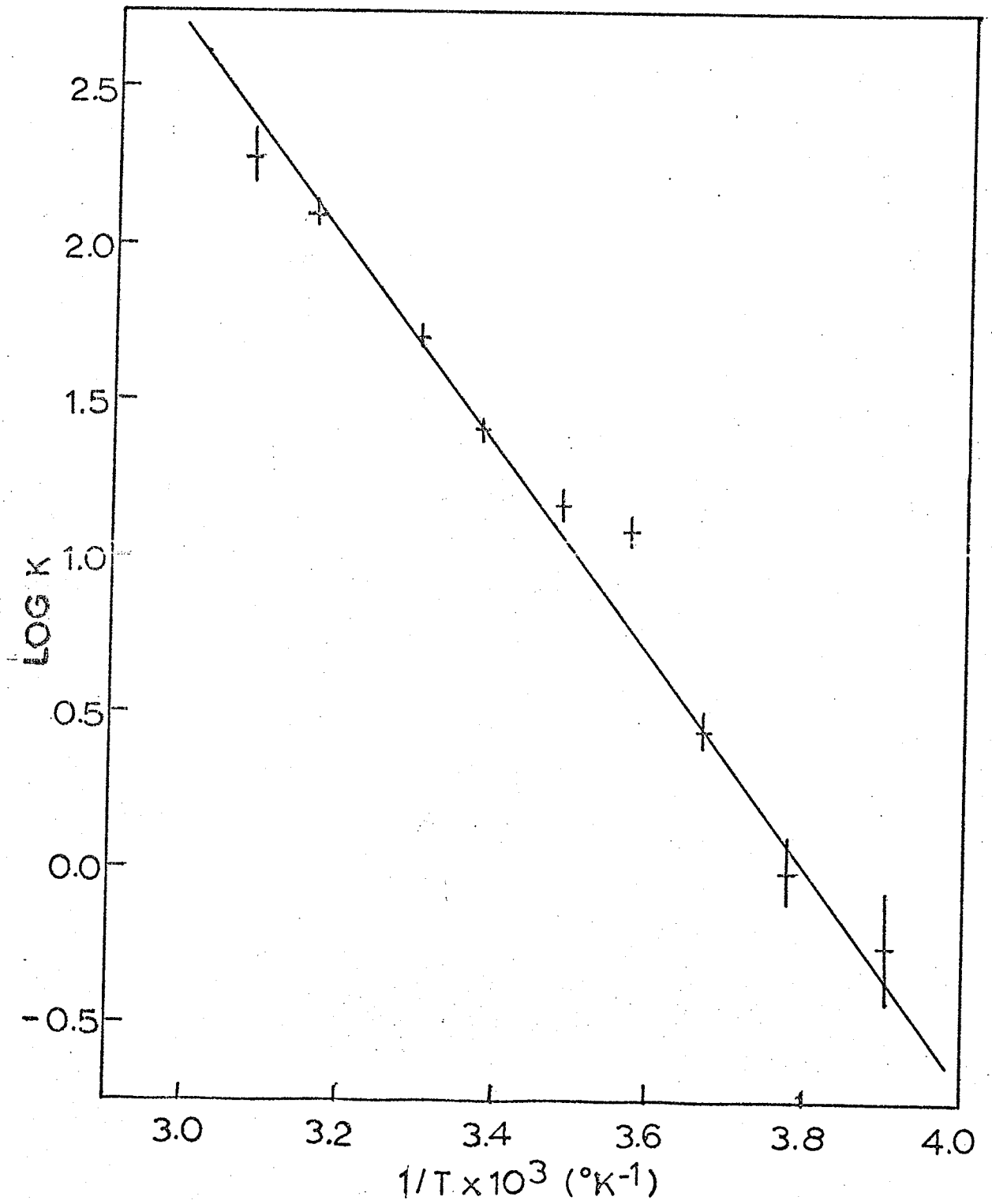
2.5
2.0
1.5
1.0
0.5
0.0
-0.5
LOG K
3.0
3.2
3.4
3.6
3.8
4.0
1/T x 10³ (°K⁻¹)

2. Calculation of Activation Parameters

The Arrhenius parameters, E_A and log A have already been calculated. The "best" values reflect the incorporation of a reasonable T_2 estimation and a correction for the variation in relative shift with temperature. These values are listed in Table XII.

The enthalpies and entropies of activation were determined by the following two methods:

(a) Equations (2-18) and (2-19) were used. The values were calculated at 303.5°K for the toluene-d_8 solution and at 303.9°K for the MeC_6H_{11} solution since these temperatures were close to the coalescence point where measureable exchange was occurring.

(b) Plots of $\log\left(\frac{k}{T}\right)$ versus $\frac{1}{T}$ were made (4) from which the enthalpies and entropies could be calculated.

The free energies of activation were calculated from the Eyring equation (2-15) at 303.5°K for the toluene-d_8 solution and at 303.9°K for the MeC_6H_{11} solution.

A complete list of all the activation parameters for both solvents with various error estimates is given in Table XII.

TABLE XII

Summary of activation parameters.

ACTIVATION PARAMETER	Toluene-d_8 VALUE	ERRORS *		MeC_6H_{11} VALUE	ERRORS	
E_A (kcal/mole)	15.2	± 0.2	1.4	14.3	± 0.6	1.3
		0.5	1.3		1.2	2.2
log A	12.7	± 0.2	1.0	12.0	± 0.5	1.7
$\Delta G^{\neq}$ (kcal/mole)	14.9 (at 303.5°K)	± 0.1	0.1	15.0 (at 303.9°K)	± 0.2	0.1
$\Delta H^{\neq}$ (kcal/mole)	a.14.6	± 0.2	1.4	a.13.7	± 0.6	1.3
		0.5	1.3		1.2	2.2
	(at 303.5°K)			(at 303.9°K)		
	b.14.6	± 0.2	1.3	b.13.7	± 0.6	2.2
$\Delta S^{\neq}$ (e.u.)	a.-3.7 (at 303.5°K)	± 0.7	4.4	a.-7.1 (at 303.9°K)	± 2.2	7.8
	b.-1.1	± 0.7	4.4	b.-4.4	± 2.2	7.8

* First error column contains the standard error and 90% confidence limits; second column contains max. and min. slopes error and T_2 error. When only two errors are listed, first column contains standard error and second the T_2 error.

3. Errors

The errors in the activation parameters were estimated in three ways. The first way was a statistical method in which both standard errors and 90% confidence limits were calculated (43). The errors in E_A and $\Delta H^{\neq}$ were based on the standard error in estimating the slope of the straight line in the least squares analysis. The errors in log A and $\Delta S^{\neq}$ were based on the standard error in the intercept, while those for $\Delta G^{\neq}$ depended upon the standard error in estimating log k.

The second way of calculating errors was based on the difference between the maximum and minimum slopes of the straight lines which could be drawn through the given set of points. Assuming that all input parameters were correct, the error in the lifetime would arise from errors in obtaining the widths of the various peaks in the experimental spectra. In the intermediate to fast exchange region these width errors were standard deviations from the mean. Thus from the two extreme values of $\Delta\nu_{\frac{1}{2}}$, the errors in log k were estimated. The difference between these two values corresponded to the maximum uncertainty in log k for a given temperature. In the slow exchange region the uncertainties were obtained from the large range of k values in which every experimental linewidth would match with the calculated linewidths. These errors in log k are indicated by vertical lines drawn through the points in figures 7 and 8. The uncertainty in temperature, assumed to be $\pm$ 1°C, is also shown on the plots by a horizontal line through each point. Therefore

the total uncertainty is represented by a rectangle. Two straight lines, pivoting about the coalescence temperature, were drawn in such a manner as to pass through almost every rectangle (44,45). From the difference in the slopes of these two lines was obtained an estimation of the error in the activation energy.

Finally, the error introduced by the effective T_2 has already been calculated in the preceding section. All the error estimates are listed in Table XII.

Comparing these results, it is seen that the statistical estimations are fairly small whereas the systematic errors introduced by the uncertainties in log k and in T_2 are much larger. It is felt that in all NMR rate determinations estimates of the systematic errors involved should be made. Far too many results have been reported with only standard errors listed, and these are probably much too optimistic.

B. Mechanism for the Hindered Rotation

From the spectra of pentachlorotoluene at -40°C (figures 1 and 2), a mechanism for the hindered rotation is now proposed. It may be represented by the following equilibrium equation:

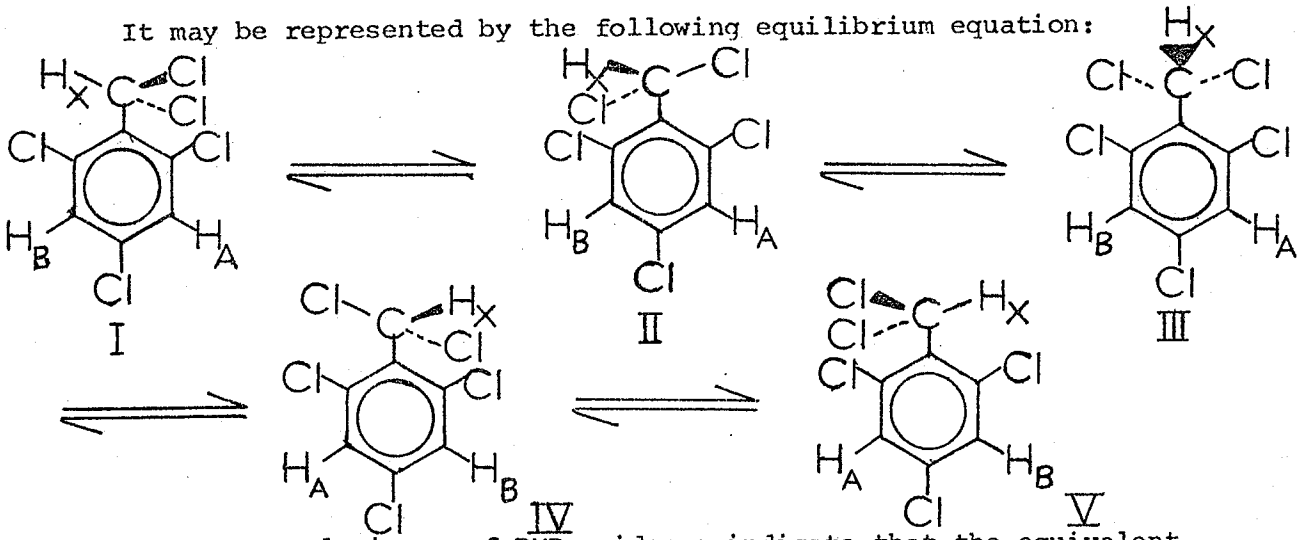

Several pieces of PMR evidence indicate that the equivalent conformers, I and V, represent the ground states for the rate process. First of all, the low field shift of the H_X resonance may be attributed to these conformers. Since the methine proton lies in the plane of the ring, it is strongly deshielded by the magnetic anisotropy and by hydrogen-bonding to the ortho-chlorine atom (35). Secondly, a large five-bond coupling of 0.50 H_z was observed between H_A and H_X, but only a very small coupling (< 0.1 H_z) was observed (indicated by the broadness of the peaks) between H_B and H_X. Examples of such stereospecific coupling have been noted before (36) in such compounds as vinyl formate (46) and ortho-hydroxy benzaldehydes (47). It was concluded that it is the "straightest" zig-zag path which results in the largest coupling (36). Finally, in tetrachlorotoluene no coupling was

observed between the methine proton and the para ring proton (35). This fact is again consistent with the molecule's spending most of its time in conformations I or V. The lifetimes of the other conformers must be very small at low temperatures or else some para coupling via the hyperconjugative mechanism (48) would have been observed.

Rotation of the dichloromethyl group is severely restricted at low temperatures due to steric hindrance between the sidechain and ring chlorine atoms and by hydrogen-bonding between the methine proton and the ortho-chlorine atom (35). The equivalent conformers II and IV in which the chlorine atoms are eclipsed,are the most sterically hindered of the intermediate states and probably represent the transition states. Conformer III is somewhat less sterically hindered and as such will have a slightly lower energy. The ground states, I and V, will be stabilized by the hydrogen-bonding and will have the lowest energy. The proposed free energy change for the rotational process is represented graphically in figure9. As can be seen from this diagram, the free energy difference between the transition states and conformer III is very small compared to that between the ground and transition states.Therefore once the molecule is in transition state II, the probability of its returning to ground state I or continuing across the barrier to ground state V will be the same. For this reason the transmission coefficient used to calculate the free energy and entropy of activation was taken to be 1/2.

FIGURE 9

A graphical representation of the free energy change for the hindered rotation in pentachlorotoluene.

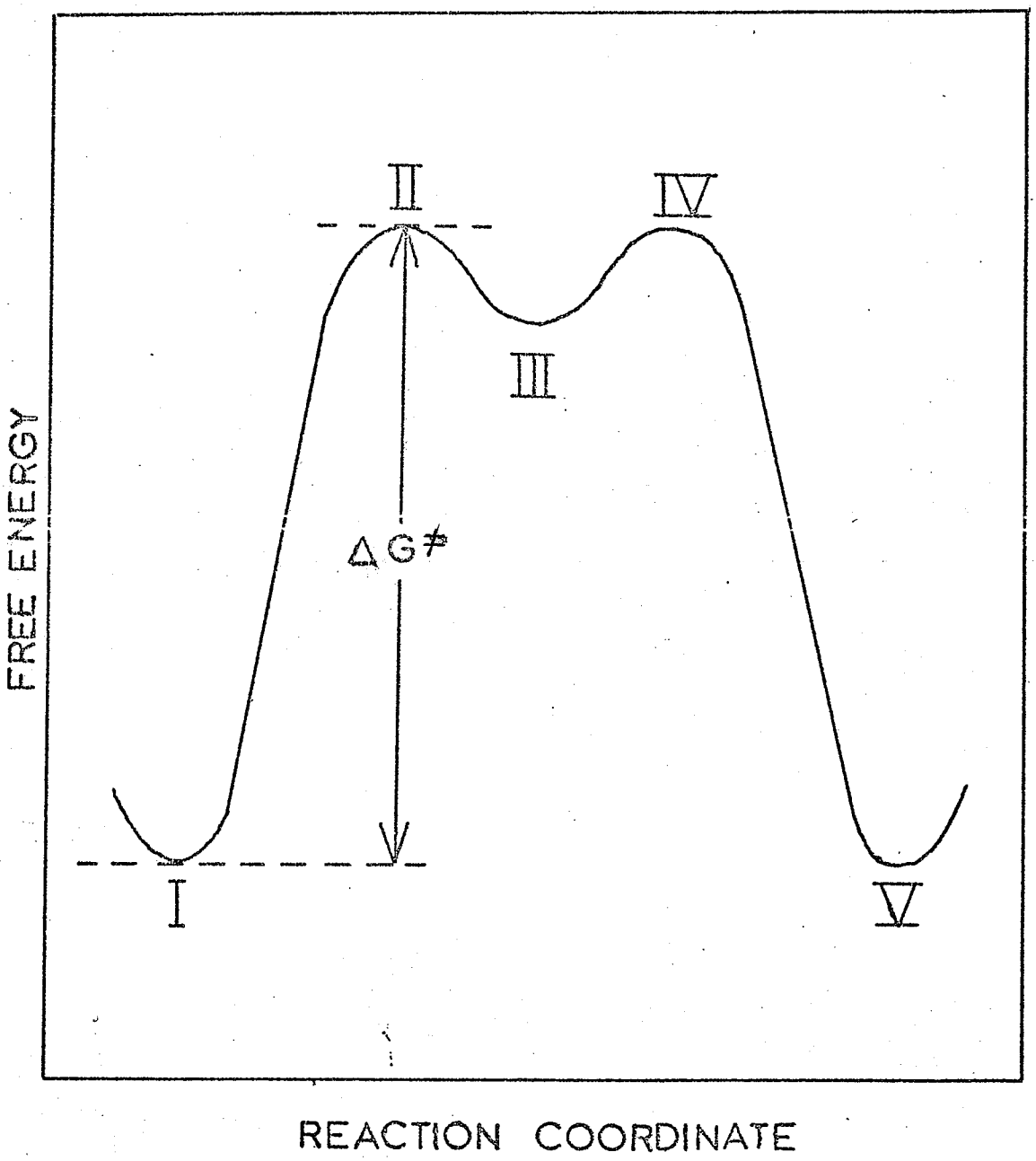
II
IV
III
ΔG≠
I
V
FREE ENERGY
REACTION COORDINATE

In a recent study of the conformation of 1,3,5-trimethyl-2-isopropylbenzene (49), the ground and transition state conformers chosen were completely analogous to the ones chosen in the present study.

The broadening of the AB portion of the spectrum as the compound was heated (figures 5 and 6) was evidence that the dichloromethyl group was beginning to flip from conformations I to V at an appreciable rate. As a result the environments of the ring protons were being interchanged. The single broad peak observed at the coalescence temperature indicated that the rate of rotation of the dichloromethyl group was comparable to the chemical shift difference between the two ring protons. The sharp doublet due to the ring protons at about 70°C indicated that rotation was fast enough so as to cause H_A and H_B to experience the same average environment. The coupling of H_X to H_A and H_B was also an average, $\frac{1}{2}$ (0.5 + 0.1) H_Z, if it is assumed that J_{BX} is about 0.1 H_Z.

The methine resonance peak experienced no similar broadening as the rotational rate was varied since the environment of this proton was identical in both ground state conformations. The signal merely changed from a sharp doublet due to the stereospecific coupling at slow exchange, to a sharp triplet due to the average coupling at fast exchange.

The values obtained for the activation energy and enthalpy (Table XII) were fairly large. This high barrier is probably the result of steric effects and of hydrogen-bonding (35). Another

contribution to the barrier may be hyperconjugation between the sidechain chlorine atoms and the Π system (35,50).

The values of the free energy of activation for the toluene-d_8 and MeC_6H_{11} solutions were within standard error of each other. The small deviation in this parameter was not unexpected (29). Moreover these values were in good agreement with that estimated (15 ± 1 kcal/mole at 25°C) for tetrachlorotoluene (35).

Finally the relatively low frequency factors and negative entropies obtained in this work deserve some comment. So-called "normal" frequency factors are usually considered to lie near log A = 13.0 and associated entropies are small and positive (51). A good discussion of the sign of the entropy in terms of a three-dimensional potential energy diagram has been given in reference (52). In essence it was stated that a negative entropy indicates that the reaction path is very constrained and that there are very few degrees of freedom in the transition state. In pentachlorotoluene, as pointed out previously, the transition state must be very sterically hindered and as such will have very few degrees of freedom. Therefore negative entropy values should not be unexpected. However the systematic errors associated with the entropy values obtained in this work were all larger than the value itself and so too much significance should not be placed on the negative sign.

C. Summary and Conclusions

A proton magnetic resonance study of the rate process involving the hindered rotation of the dichloromethyl group in α,α,2,4,6-pentachlorotoluene was carried out using the complete line-shape method.

Temperature studies in the range, -40° to 70°C were performed on the compound in two solvents, toluene-d_8 and methylcyclohexane. The spectra at -40°C were analyzed using standard ABX procedures. The unusually large five-bond stereospecific coupling between the methine proton and only one of the ring protons followed the zig-zag rule. The difference in the relative chemical shift of the ring protons between the two solvents was a result of the aromatic solvent induced shift.

Rate constants were determined by matching the linewidths at half-height of the resonance peaks of the experimental spectra to those which were calculated as a function of lifetime by computer. The procedure was complicated by the fact that an effective relaxation time was difficult to determine and that the relative chemical shift of the ring protons in the toluene-d_8 solution varied with temperature. An effective relaxation time was finally deduced from the linewidth of the impurity peak due to hexachlorotoluene, and the variation in shift was accounted for by an extrapolation from low temperatures.

The various activation parameters for the hindered rotation were calculated from Arrhenius plots and from absolute reaction rate theory. They are listed in Table XII. The values obtained

for the toluene-d_8 and methylcyclohexane solutions were in reasonable agreement when the variation in chemical shift was taken into account. Both statistical and systematic error limits were estimated for these parameters, and it was concluded that all future rate studies should not be considered complete without some indication of the systematic errors involved.

Finally a mechanism was proposed for the rotation of the dichloromethyl group. Various pieces of evidence were put forward to show that the ground state conformation of the molecule is that in which the methine proton lies in the plane of the ring. The chlorine atoms are eclipsed in the transition state. It was concluded that the main contributions to the energy barrier were steric hindrance and hydrogen-bonding and that the negative entropy values were the result of the constrained transition state.

D. Suggestions for Future Research

A temperature study was undertaken for pentachlorotoluene in CS_2, but since the slow exchange spectrum was an ABC system, rates could not be determined with the present computer program. An obvious extension of this work would be a rate study for this solution using an ABC exchange program.

Work needs to be done on various derivatives of pentachlorotoluene. Other halogens or nitro groups could be substituted for one or more of the chlorines. Then the difference in activation parameters could be interpreted in terms of steric and charge effects.

Finally the present study could be repeated on a 100 MH_z spectrometer. This would almost double the relative shift of the ring protons and thus provide a good check for the present results.

APPENDIX I

Density Matrix Equations

Complete derivations of the equations shown here may be found in references (21-23).

The average value of some observable Q in state $|\psi\rangle$ is given by

$$\langle Q \rangle = \langle \psi_k | Q | \psi_k \rangle \qquad \text{(A-1)}$$

If $|\psi_k\rangle$ is expanded in terms of a complete set of orthonormal basis functions ϕ_i as

$$|\psi_k\rangle = \sum_i c_{ki} \phi_i \qquad \text{(A-2)}$$

then equation (A-1) becomes

$$\langle Q \rangle = \sum_{i,j} c^*_{ki} c_{kj} \langle \phi_i | Q | \phi_j \rangle \qquad \text{(A-3)}$$

The density matrix element ρ_{ji} is defined by

$$\rho_{ji} = c^*_{ki} c_{kj} \qquad \text{(A-4)}$$

Therefore the average value of Q may be written as

$$\langle Q \rangle = \mathrm{Tr}(\rho Q) = \mathrm{Tr}(Q\rho) \qquad \text{(A-5)}$$

where ρ and Q are the matrix representatives of their respective operators in the basis ϕ_i.

The relation describing the time-dependence of the density matrix operator is

$$\frac{d\rho}{dt} = \frac{i}{\hbar}\left[\rho, \mathcal{H}\right] \qquad \text{(A-6)}$$

where $\mathcal{H}$ is the Hamiltonian for the system.

For a spin system at thermal equilibrium, an explicit expression for the operator ρ is

$$\rho = \frac{e^{-\mathcal{H}/kT}}{\sum_i e^{-E_i/kT}} \qquad \text{(A-7)}$$

This equation holds when the ϕ_i's are eigenfunctions of $\mathcal{H}$ and the E_i's are their corresponding eigenvalues.

APPENDIX II

Matrices required for Exchanging AB Line-shape Derivation

For a derivation of the equations contained here see references (20,26).

The exchange term is

$$\left(\frac{d\rho}{dt}\right)_{exch} = \frac{1}{\tau}\begin{bmatrix} 0 & \rho_{13} - \rho_{12} & \rho_{12} - \rho_{13} & 0 \\ \rho_{31} - \rho_{21} & \rho_{33} - \rho_{22} & \rho_{32} - \rho_{23} & \rho_{34} - \rho_{24} \\ \rho_{21} - \rho_{31} & \rho_{23} - \rho_{32} & \rho_{22} - \rho_{33} & \rho_{24} - \rho_{34} \\ 0 & \rho_{43} - \rho_{42} & \rho_{42} - \rho_{43} & 0 \end{bmatrix} \quad \text{(A-8)}$$

The relaxation term is

$$\left(\frac{d\rho}{dt}\right)_{relax} = \begin{bmatrix} \frac{(\rho_o - \rho)_{11}}{T_1} & -\frac{\rho_{12}}{T_2} & -\frac{\rho_{13}}{T_2} & -\frac{\rho_{14}}{T_2} \\ -\frac{\rho_{21}}{T_2} & \frac{(\rho_o - \rho)_{22}}{T_1} & -\frac{\rho_{23}}{T_2} & -\frac{\rho_{24}}{T_2} \\ -\frac{\rho_{31}}{T_2} & -\frac{\rho_{32}}{T_2} & \frac{(\rho_o - \rho)_{33}}{T_1} & -\frac{\rho_{34}}{T_2} \\ -\frac{\rho_{41}}{T_2} & -\frac{\rho_{42}}{T_2} & -\frac{\rho_{43}}{T_2} & \frac{(\rho_o - \rho)_{44}}{T_1} \end{bmatrix} \quad \text{(A-9)}$$

Evaluation of the commutation relationship in equation (2-12) requires a knowledge of the Hamiltonian. The form of this Hamiltonian in a reference frame rotating at angular frequency ω about the stationary field H_o is

$$\mathcal{H} = \mathcal{H}^o + \mathcal{H}' + \mathcal{H}^t$$

where $\mathcal{H}^o = \left[\gamma H_o(1-\sigma_1) - \omega\right] I_z(1) + \left[\gamma H_o(1-\sigma_2) - \omega\right] I_z(2)$

$$\mathcal{H}' = J\underline{I}(1)\cdot\underline{I}(2)$$

$$\mathcal{H}^t = \gamma H_1\left[I_x(1) + I_x(2)\right]$$

and σ_1 and σ_2 are the shielding constants for the A and B nuclei respectively, J is the coupling constant, and $\underline{I}(1)$ and $\underline{I}(2)$ are the

spin angular momentum operators for the nuclei.

The four required matrix elements of the commutation relationship $\left[\rho, \mathcal{H}^{o} + \mathcal{H}'\right]$ are

$$\begin{aligned}
\left[\rho, \mathcal{H}^{o} + \mathcal{H}'\right]_{21} &= (-\Delta - \tfrac{1}{2}\delta + \tfrac{1}{2}J)\rho_{21} - \tfrac{1}{2}J\rho_{31} \\
\left[\rho, \mathcal{H}^{o} + \mathcal{H}'\right]_{31} &= (-\Delta + \tfrac{1}{2}\delta + \tfrac{1}{2}J)\rho_{31} - \tfrac{1}{2}J\rho_{21} \\
\left[\rho, \mathcal{H}^{o} + \mathcal{H}'\right]_{42} &= (-\Delta + \tfrac{1}{2}\delta - \tfrac{1}{2}J)\rho_{42} + \tfrac{1}{2}J\rho_{43} \\
\left[\rho, \mathcal{H}^{o} + \mathcal{H}'\right]_{43} &= (-\Delta - \tfrac{1}{2}\delta - \tfrac{1}{2}J)\rho_{43} + \tfrac{1}{2}J\rho_{42}
\end{aligned} \qquad \text{(A-10)}$$

where $\Delta = \omega - \tfrac{1}{2}\gamma H_{o}(2-\sigma_{1}-\sigma_{2})$

$\delta = \gamma H_{o}(\sigma_{2}-\sigma_{1}) \equiv$ chemical shift difference between H_{A} and H_{B} resonance peaks.

Using certain approximations (19), the complete matrix for $\left[\rho, \mathcal{H}^{t}\right]$ is

$$\left[\rho, \mathcal{H}^{t}\right] = C \begin{bmatrix} 0 & -1 & -1 & 0 \\ 1 & 0 & 0 & -1 \\ 1 & 0 & 0 & -1 \\ 0 & 1 & 1 & 0 \end{bmatrix} \qquad \text{(A-11)}$$

where $C = \dfrac{\gamma^{2}\hbar H_{o}H_{1}}{2NkT}$ and $N = \sum_{i} e^{-E_{i}/kT}$

BIBLIOGRAPHY

1. C.S. Johnson, Jr. In "Advances in Magnetic Resonance", Vol. 1, J.S. Waugh (Editor), Academic Press Inc.,New York, 1965.

2. L.W. Reeves. In"Advances in Physical Organic Chemistry", Vol. 3, V. Gold (Editor), Academic Press Inc., New York, 1965.

3. J.J. Delpuech. Bull. Soc. Chim. France, 2697 (1964).

4. G. Binsch. In "Topics in Stereochemistry", Vol. 3, E.L. Eliel and N.L. Allinger (Editors), John Wiley & Sons Inc., New York, 1968.

5. A. Carrington and A.D. McLachlan. "Introduction to Magnetic Resonance", Harper and Row, New York, 1967.

6. J.A. Pople, W.G. Schneider and H.J. Bernstein. "High Resolution Nuclear Magnetic Resonance", McGraw-Hill Book Co. Inc., New York, 1959.

7. J.W. Emsley, J. Feeney and L.H. Sutcliffe. "High Resolution Nuclear Magnetic Resonance", Vol. 1, Pergamon Press Ltd., Oxford, 1965.

8. F. Bloch. Phys. Rev. 70, 460 (1946).

9. H.S. Gutowsky, D.W. McCall and C.P. Slichter. J. Chem. Phys. 21, 279 (1953).

10. H.S. Gutowsky and A. Saika. J. Chem. Phys. 21, 1688 (1953).

11. H.S. Gutowsky and C.H. Holm. J. Chem. Phys. 25, 1288 (1956).

12. H.M. McConnell. J. Chem. Phys. 28, 430 (1958).

13. M.T. Rogers and J.C. Woodbrey. J. Phys. Chem. 66, 540 (1962).

14. L. Piette and W.A. Anderson. J. Chem. Phys. 30, 899 (1959).

15. E. Grunwald and A. Loewenstein. J. Chem. Phys. 27, 630 (1957).

16. S. Meiboom, Z. Luz and D. Gill. J. Chem. Phys. 27, 411 (1957).

17. K. Dahlqvist and S. Forsén. J. Phys. Chem. 69, 4062 (1965).

18. J. Kaplan. J. Chem. Phys. 28, 278 (1958); 29, 492 (1958).

19. S. Alexander. J. Chem. Phys. 37, 967, 974 (1962).

20. G.M. Whitesides. Ph.D. Thesis, California Institute of Technology, 1964.

21. U. Fano. Rev. Mod. Phys. 29, 74 (1957).

22. C.P. Slichter. "Principles of Magnetic Resonance", Harper & Row, New York, 1963.

23. R.M. Lynden-Bell. In "Progress in Nuclear Magnetic Resonance Spectroscopy", Vol. 2, J.W. Emsley, J. Feeney and L.H. Sutcliffe, (Editors), Pergamon Press Ltd., Oxford, 1967.

24. C.S. Johnson. J. Chem. Phys. 41, 3277 (1964).

25. R.A. Newmark and C.H. Sederholm. J. Chem. Phys. 43, 602 (1965).

26. B.W. Goodwin. Master's Thesis, University of Manitoba, 1969.

27. K.J. Laidler. "Chemical Kinetics", McGraw-Hill Book Co. Inc., New York, Second Edition, 1965.

28. A. Allerhand, H.S. Gutowsky, J. Jonas and R.A. Meinzer. J. Am. Chem. Soc. 88, 3185 (1966).

29. A. Allerhand, F.M. Chen and H.S. Gutowsky. J. Chem. Phys. 42, 3040 (1965).

30. M. Jautelat and J.D. Roberts. J. Am. Chem. Soc. 91, 642 (1969).

31. M. Rabinovitz and A. Pines. J. Am. Chem. Soc. 91, 1585 (1969).

32. T.H. Siddall III and W.E. Stewart. J. Phys. Chem. 73, 40 (1969).

33. J. White and R. Adams. J. Am. Chem. Soc. 54, 2104 (1932).

34. F.D. Chattaway and R.C.T. Evans. J. Chem. Soc. 69, 848 (1896).

35. T. Schaefer, R. Schwenk, C.J. Macdonald and W.F. Reynolds. Can. J. Chem. 46, 2187 (1968).

36. C.N. Banwell and N. Sheppard. Discussions Faraday Soc. 34, 115 (1967).

37. J. Gerig and J.D. Roberts. J. Am. Chem. Soc. 88, 2791 (1966).

38. F.A.L. Anet and A.J.R. Bourn. J. Am. Chem. Soc. 89, 760 (1967).

39. G. Binsch and J.D. Roberts. J. Am. Chem. Soc. 87, 5157 (1965).

40. M.E.C. Biffin, L. Crombie, T.M. Connor and J.A. Elvidge. J. Chem. Soc. (B) 841 (1967).

41. P. Lazlo. In "Progress in Nuclear Magnetic Resonance Spectroscopy", Vol. 3, J.W. Emsley, J. Feeney and L.H. Sutcliffe (Editors), Pergamon Press Ltd., Oxford, 1967.

42. R.J. Schwenk. Master's Thesis, University of Manitoba, 1968.

43. J.E. Freund, P.E. Livermore and I. Miller. "Manual of Experimental Statistics", Prentice-Hall Inc., Englewood Cliffs, N. J., 1960.

44. A. Mannschreck, A. Mattheus and G. Rissmann. J. Mol. Spectry. 23, 15 (1967).

45. H.G. Schmid, H. Friebolm, S. Kabuss and R. Mecke. Spectrochim. Acta. 22, 623 (1966).

46. T. Schaefer. J. Chem. Phys. 36, 2235 (1962).

47. V.J. Kowalewski and D.G. Kowalewski. personal communication.

48. D.J. Blears, S.S. Danyluk and T. Schaefer. Can. J. Chem. 46, 654 (1968).

49. A. Mannschreck and L. Ernst. Tetrahedron Letters. 57, 5939. (1968)

50. K. Kimura and S. Nagakura. J. Chem. Phys. 47, 2916 (1967).

51. R.C. Neuman, D.N. Roark and V. Jonas. J. Am. Chem. Soc. 89, 3412 (1967).

52. G. Kotowycz. Ph.D. Thesis, University of Manitoba, 1967.